

Fast deposition of plasma polymer layers

Citation for published version (APA):

Beulens, J. J., Kroesen, G. M. W., Schram, D. C., Timmermans, C. J., Crouzen, P. C. N., Vasmel, H., Schuurmans, H. J. A., Beijer, C. B., & Werner, J. (1990). Fast deposition of plasma polymer layers. *Journal of Applied Polymer Science: Applied Polymer Symposium*, 46, 527-540.

Document status and date:

Published: 01/01/1990

Document Version:

Publisher's PDF, also known as Version of Record (includes final page, issue and volume numbers)

Please check the document version of this publication:

- A submitted manuscript is the version of the article upon submission and before peer-review. There can be important differences between the submitted version and the official published version of record. People interested in the research are advised to contact the author for the final version of the publication, or visit the DOI to the publisher's website.
- The final author version and the galley proof are versions of the publication after peer review.
- The final published version features the final layout of the paper including the volume, issue and page numbers.

[Link to publication](#)

General rights

Copyright and moral rights for the publications made accessible in the public portal are retained by the authors and/or other copyright owners and it is a condition of accessing publications that users recognise and abide by the legal requirements associated with these rights.

- Users may download and print one copy of any publication from the public portal for the purpose of private study or research.
- You may not further distribute the material or use it for any profit-making activity or commercial gain
- You may freely distribute the URL identifying the publication in the public portal.

If the publication is distributed under the terms of Article 25fa of the Dutch Copyright Act, indicated by the "Taverne" license above, please follow below link for the End User Agreement:

www.tue.nl/taverne

Take down policy

If you believe that this document breaches copyright please contact us at:

openaccess@tue.nl

providing details and we will investigate your claim.

FAST DEPOSITION OF PLASMA POLYMER LAYERS

J.J. BEULENS, G.M.W. KROESEN,
D.C. SCHRAM, and C.J. TIMMERMANS

*Department of Physics,
Eindhoven University of Technology,
POB 513, 5600 MB Eindhoven,
The Netherlands*

P.C.N. CROUZEN, H. VASMEL,
H.J.A. SCHUURMANS, C.B. BEIJER,
and J. WERNER

*Shell Research, POB 3003,
1003 AA Amsterdam,
The Netherlands*

SYNOPSIS

In a combined effort of the Eindhoven University of Technology and Shell Research Laboratories Amsterdam the potential of a new plasma deposition method for polymer deposition has been investigated. In this method a high pressure plasma arc is expanded into a vacuum chamber. The monomer is injected either in the arc or in the vacuum chamber. At pressures around 1 mbar a directed beam is formed leading to high deposition rates at areas of 100 cm². At lower pressures the plasma is evenly distributed and lower rates for larger areas are the result. Several characteristics of the deposition (as rate etc.) have been measured. Special attention has been devoted to the

relation between power load on the substrate and the useful particle load. The thickness is determined by He-Ne ellipsometry, and characteristics of the layers by IR and visible ellipsometry.

INTRODUCTION

Plasma polymerization is a specific branch of plasma deposition. In the material deposited a very special cross linking arises, which is a direct consequence of the relatively high energy of the impinging particles. It resembles classical polymerization as such that the layer grows from linkage of monomer particles. It differs, however, largely in the extent that there is only short range order combined with a high cross linking density. In so far it can also be regarded as amorphous material with dangling bonds neutralized with (usually) H-atoms. These layers have very specific properties and are used in many applications. The hard layers can be used as protective materials in passivation layers. Other type of layers serve as selective layers in e.g. membrane technology [2,1]. In the latter application fast growth is essential while maintaining the excellent material properties, in order to eventually arrive at acceptable production costs.

In earlier work a new approach is developed to reach these higher rates of deposition [3]. The principle is to separate the plasma production from the plasma treatment. One advantage of this method is that the plasma existence demands (the plasma is a non equilibrium system) no longer limit the maximum fluxes at the substrate. Connected to this advantage is that the ratio of useful particle flux and power flux to the substrate can be appreciably higher. This fulfills the requirements to reach higher deposition rates at moderate power fluxes. In deposition of carbon based hard materials on Si substrates rates of 100 nm/s have been reached. This is accompanied by C fluxes of $5 \cdot 10^{21}/m^2s$ and power fluxes of $5 \cdot 10 \cdot 10^4 W/m^2$. Even though this is already a favorable ratio of particle flux and power flux, the power flux is too high for soft materials, because they will melt at these high

power loads. In the course of the present work a detailed study has been undertaken to investigate the dependencies of particle and power fluxes on the parameters of the deposition process and the relation with the quality of the deposited layers.

DESCRIPTION OF APPARATUS AND MODES OF OPERATION

A detailed sketch of the deposition apparatus is shown in Fig. 1. At the left is the plasma production section which consists of a relatively high pressure (0.1-1 atm.) cascade arc with a bore of 4 mm and a length of 6 cm. Currents are in the range of 10-100 A (voltage range 50-150 V), flows are between 20-200 scc/s. The primary carrier gas is argon.

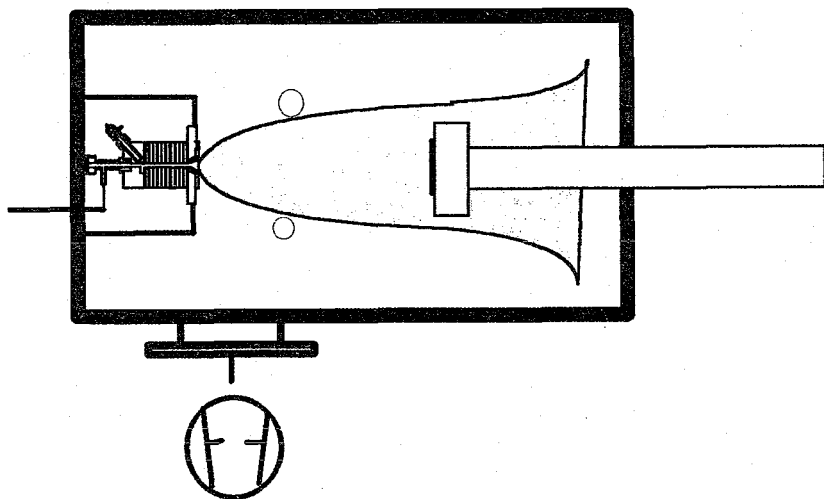


Fig 1. Outline of the reactor for plasma deposition used in these experiments. The plasma is generated in the cascaded arc and transported towards the substrat supersonic expansion and a subsonic plasma beam. The toluene is injected through a ring in the vacuum chamber and the methane is injected through the nozzle of the cascaded arc.

The resulting plasma exhibits a high degree of ionization, typically between 5-20%, and is rather close to LTE [3]. Typical electron densities and electron temperatures are $10^{22}/\text{m}^3$ and 1 eV, respectively. On the right is the deposition chamber which is evacuated to (operation) pressures around 1 mbar by two roots blowers and a rotating piston pump with a total capacity of $2600 \text{ m}^3/\text{hr}$. Using a stepper motor controlled valve, between the pumps and the chamber, the pumping speed and therefore also the chamber pressure can be kept constant or varied for constant or different gas flow rates respectively. With a diffusion pump a base pressure of 10^{-6} mbar can be reached. Because of the pressure difference the plasma will be accelerated to supersonic flow. The sonic velocity is high, as in these high density plasmas also the heavy particle temperature is high. For argon at 1 eV the sonic velocity is about $2 \cdot 10^3 \text{ m/s}$. In the deposition chamber the plasma is accelerated and strongly cooled by the supersonic expansion, passes a shock and drifts subsonically while expanding to the substrate. So the characteristics are: high density, high velocity, low electron temperature, high electron density and elevated heavy particle temperature in subsonic flow region behind the shock. In view of the high electron density, the plasma created bias potential is low, typically 1 V. This leads to low energies of the impinging ions.

There are essentially two modes of operation. In the first one, which we will call the ionic mode, a percentage monomer e.g. CH_4 is injected in the cascaded arc. The monomer is dissociated effectively and the carbon atoms, and to a lesser extent the hydrogen atoms, are charge exchanged with the argon ions. During the shock passage and expansion the recombination is weak and an intensive plasma beam impinges on the substrate. Under these conditions the power load is substantial: $5\text{-}10 \text{ W}/\text{cm}^2$. With the large fluxes ($10^{18}/\text{cm}^2$) the ratio of ion flux to power flux is still favorable compared to traditional plasma deposition methods. The deposition rate is high, up to 200 nm/s on areas of approximately 100 cm^2 . A figure of merit R is the deposition rate divided by the specific energy flux, in the quoted example $40 \text{ nm}\cdot\text{cm}^2/\text{J} = 4 \text{ mm}^3/\text{kJ}$. This is equivalent to $\sim 100 \text{ eV}/\text{deposited particle}$.

Another mode of operation is the quenched mode. In this mode the monomer is injected in a ring surrounding the emanating plasma beam in the vacuum vessel. In this case the dissociation is only partial and molecular ions and neutral in radical form are present in significant numbers. In this case an appreciable recombination through dissociate channels takes place. The deposition rate in the present arrangement is appreciably lower, up to around 20 nm/s. The specific power flux ranges from 0.1-1 W/cm². This mode is more profitable for substrates which allow only a small power load. Moreover, radicals play a more important role in the deposition process.

This paper will give results mainly on the second mode of operation.

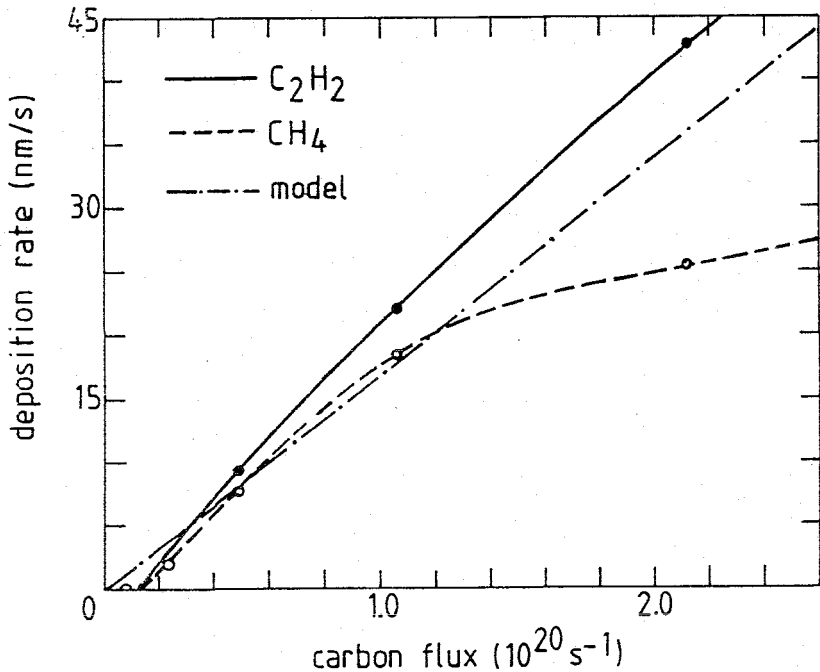


Fig 2. The deposition rate as a function of the injected number of carbon atoms for an argon plasma with an admixture of methane or acetylene. The dashed dotted curve represents calculated values [3].

EXPERIMENTAL RESULTS

First we will summarize the results on the ionic mode of operation. In fig. 2 the resulting deposition rate is plotted as function of the monomer flux: CH_4 and C_2H_2 , but saturates for CH_4 . This can be linear with the C flux for C_2H_2 . The type of material depends again on the ratio of C particles flux to power flux. This can be observed in Fig. 3 in which the refractive index is plotted as function of the so-called energy coefficient.

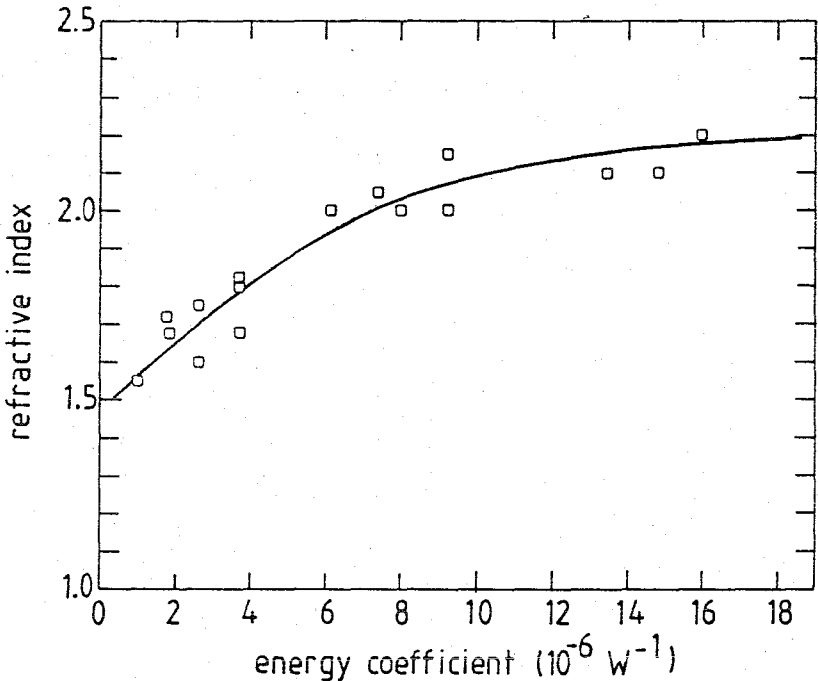


Fig 3. Plot of the refractive index, obtained by *in situ* ellipsometry, versus the energy coefficient R' defined as the ratio of the carbon flow rate (in scc/s) and the power product P (argon flow rate (in scc/s) times arc power (in W)).

This is defined as the ratio of the carbon flux and the product of arc power and argon flux.

$$R' \equiv \frac{\dot{N}_C}{\dot{N}_A \Gamma P} \quad (1)$$

This quantity is directly related to the earlier introduced quantity R , as the numerator determines the growth rate and the denominator the impinging power flux at the substrate. It is clear that soft polymeric materials with low index of refraction are deposited for low values of the ratio R' . Other material quantities can be deduced from spectroscopic ellipsometric values. A typical example is shown in Fig. 4 in which the square root of the product of absorption coefficient and energy is plotted against energy. From these data the optical band gap can be deduced, which is shown in Fig. 5.

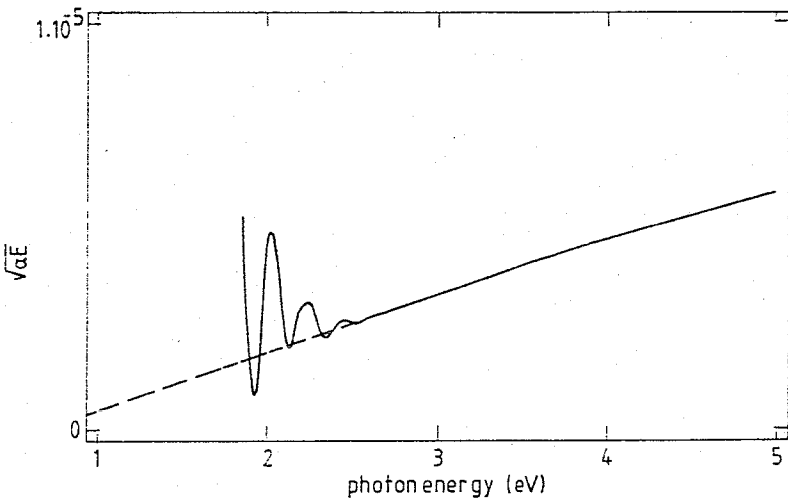


Fig 4. The Tauc parameter ($= \sqrt{\alpha E}$) as a function of photon energy.

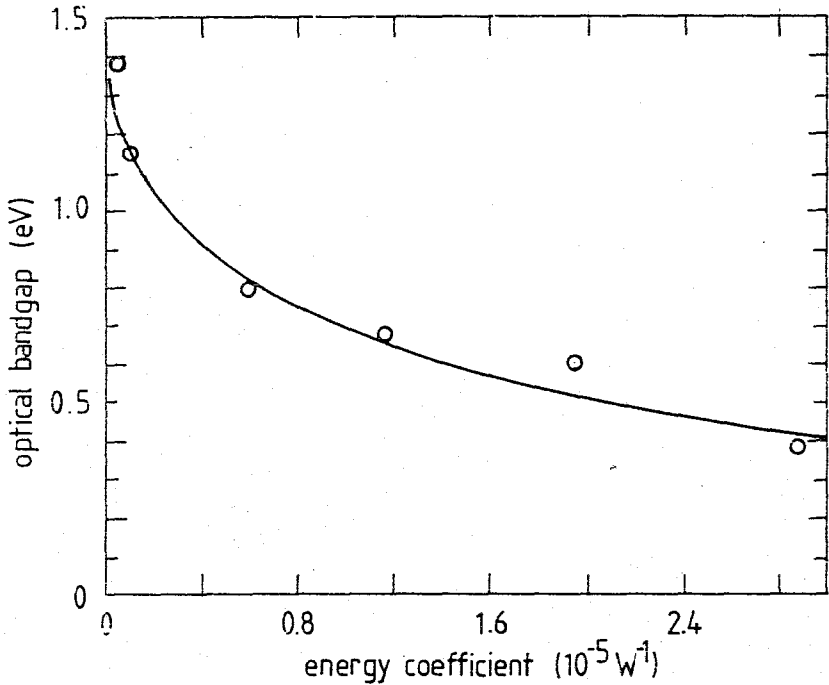


Fig 5. The optical band gap as a function of the energy coefficient R' .

The quenched mode of operation

This mode is more suited for polymer deposition on substrates with limited energy flux capability. The growth rate can still be high (10 nm/s) but is smaller than in the ionic mode. In the quenched mode a detailed study has been made of the power flux and the deposition profile. The power flux to the substrate was obtained by measuring the temperature rise of the coolant and appropriate calibration procedure. The power load on the substrate was kept low by inserting a mechanical chopper in the beam line (duty cycle 2/8, frequency about 10 Hz). The temperature of the substrate polymers was controlled between 30 and 40 °C. The deposition rate was

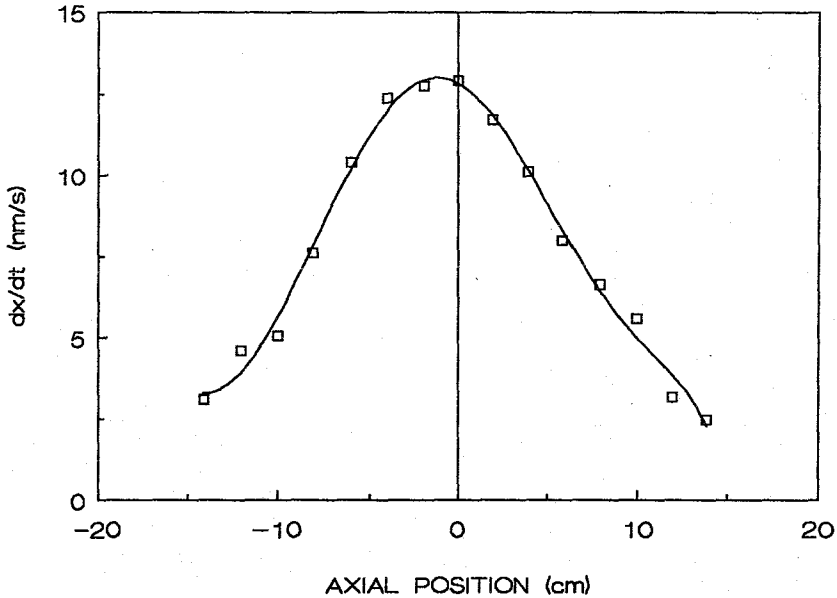


Fig 6. Typical deposition profile at a distance of 60 cm to the cascaded arc. In the figure the deposition rate is plotted vs the distance to the flow axis. Plasma settings: Argon flow rate 30 scc/s, chamber pressure 46 Pa, arc power 3.7 kW, and 0.5 ml/min (liquid) toluene flow rate.

determined by an inductive layer thickness probe and an ex situ multi-angle He-Ne ellipsometer. The monomer is toluene injected in a ring in the vacuum chamber. A typical deposition profile is shown in Fig. 6.

In Figs. 7, 8 and 9 the deposition rate, specific power flux and specific deposition rate are shown as functions of arc power, argon flow and toluene flow rate. From these figures it is clear that the specific power flux to the substrate is indeed proportional to arc power and argon flow rate and is independent of the toluene flow rate. This shows clearly the relation between the quantities R and R' .

The conclusions on this part of the work are:

1. The heat transfer to the substrate increases with the arc power and the argon flow rate in the arc.

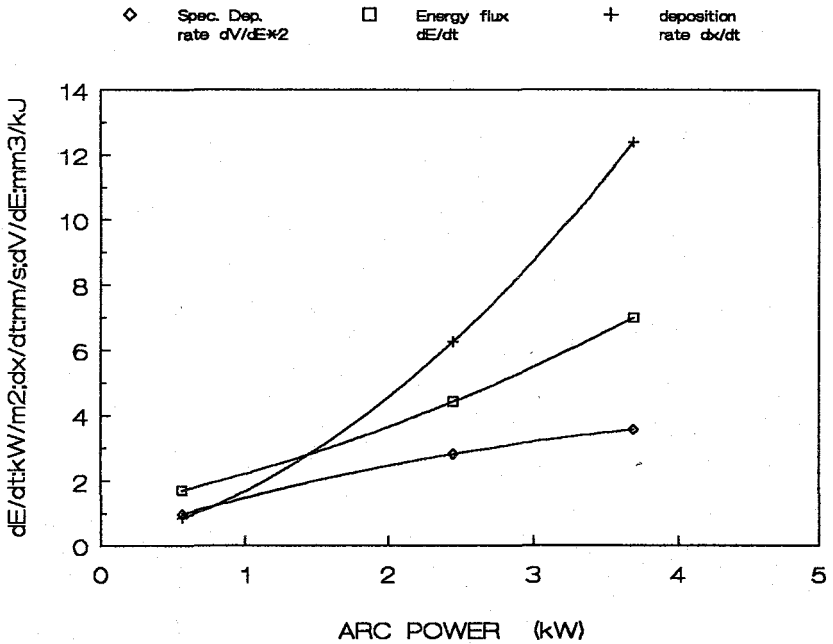


Fig 7. Deposition rate dx/dt (nm/s, crosses), energy flux dE/dt (kW/m², squares), and the specific deposition rate $dV/dE \times 2$ (mm³/kJ, diamonds), with V the deposition rate, respectively vs arc power (kW). Plasma settings: 30 scc/s argon flow rate, 0.5 ml/min toluene flow rate, 85 Pa chamber pressure.

2. The deposition rate increases with the arc power, the argon flow rate and the toluene flow rate.
3. The specific deposition rate increases strongly with arc power.

These observations can qualitatively be explained as follows. The arc injects a partially ionized plasma of 0.5-1 eV temperature. The ion fraction can charge exchange with toluene molecules leading to atomic ions or radical formation by subsequent dissociative recombination. These radicals are the active species in the deposition process. Hence higher arc power involving a higher ionization degree in the argon flow leads to a larger

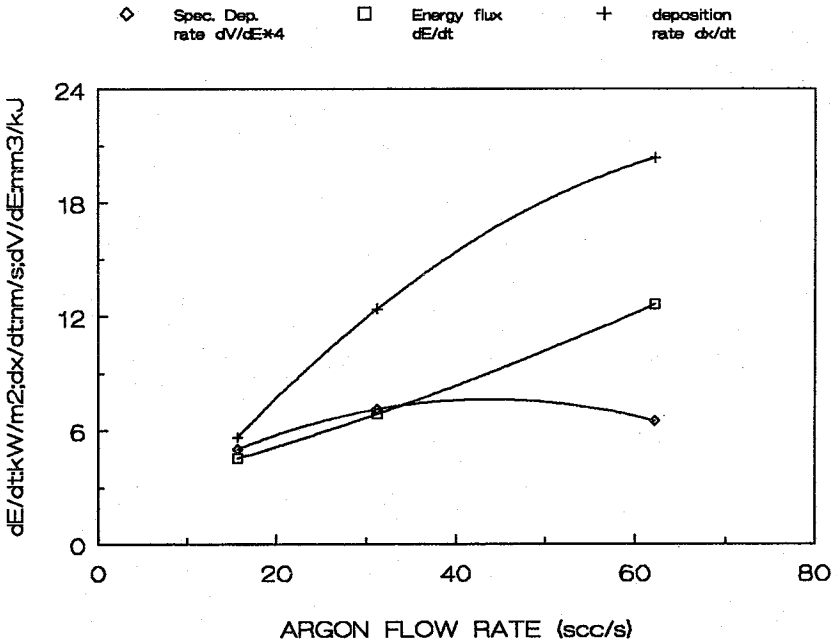


Fig 8. Deposition rate dx/dt (nm/s, crosses), energy flux dE/dt (kW/m², squares), and the specific deposition rate $dV/dE * 2$ (mm³/kJ, diamonds), with V the deposition rate, respectively vs argon flow rate (scc/s). Plasma settings: 3.6 kW arc power, 0.5 ml/min toluene flow rate, 86 Pa chamber pressure.

deposition rate.

Finally, infrared spectroscopic ellipsometry data have been obtained in some of the samples produced in this collaborative effort [4].

Fig. 10 shows the spectrum in terms of the ellipsometric angle Ψ in two wavelength ranges. The absorption peak at 1450 cm⁻¹ may refer to olefinic sp² CH₂ or to sp³ CH₂. As also a peak is found at 2946 cm⁻¹ (also : sp² CH₂) and not at 2920 cm⁻¹ (sp³ CH₂) the conclusion is that sp² CH₂ is one of the prevalent binding forms. For assignment of peaks in IR spectra see for example Dischler [5]. Absorption peaks at 1370 cm⁻¹ and 2875 cm⁻¹ can be attributed to sp³ CH and sp³ CH₃ respectively.

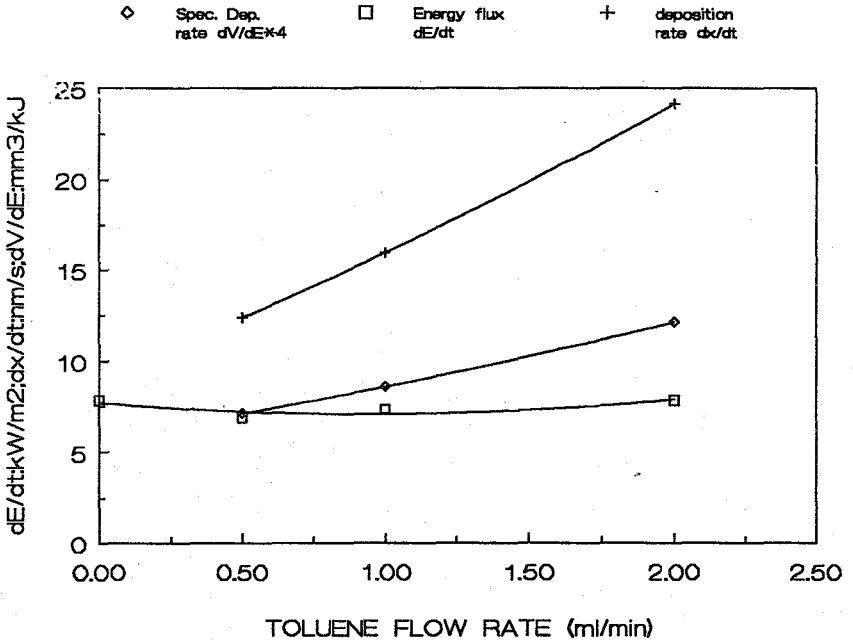


Fig 9. Deposition rate dx/dt (nm/s, crosses), energy flux dE/dt (kW/m^2 , squares), and the specific deposition rate $dV/dE \times 2$ (mm^3/kJ , diamonds), with V the deposition rate, respectively vs toluene flow rate (ml/min). Plasma settings: 30 scc/s argon flow rate, 3.7 kW arc power, 90 Pa chamber pressure.

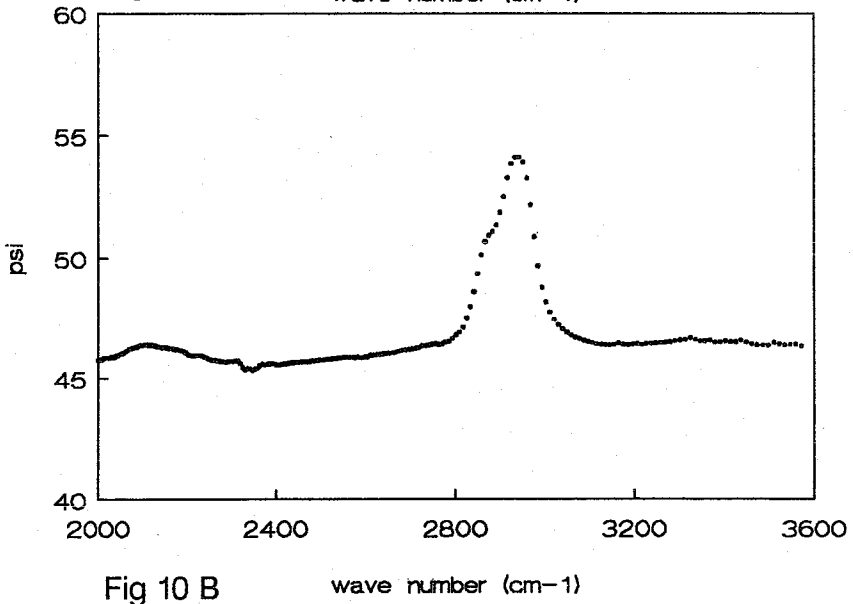
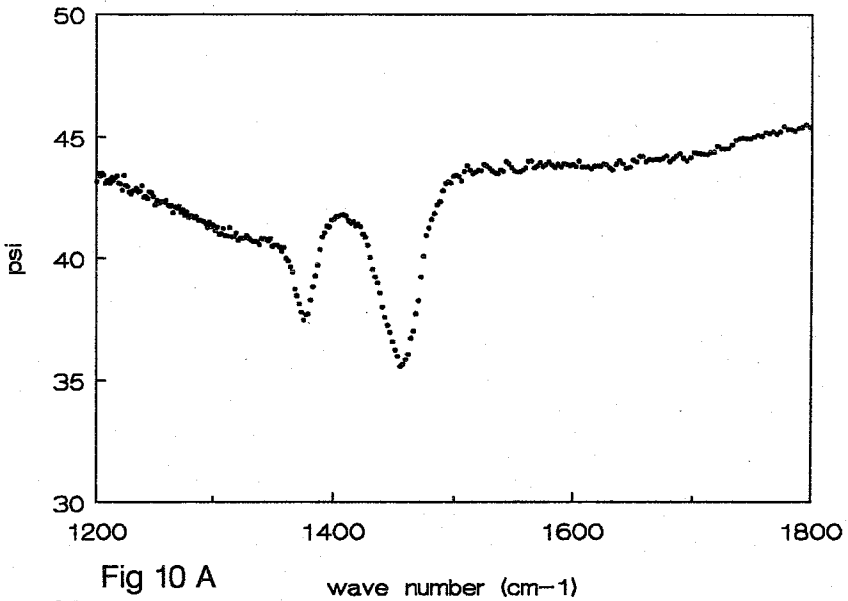


Fig 10. Ellipsometric spectra of a typical polymer like layer in two wavelength regions: A 1175-1820 cm^{-1} and B 2000-3570 cm^{-1} . Plotted are the ellipsometric angles Ψ vs wave number (cm^{-1}). The value of Ψ is strongly coupled to the absorption coefficient.

REFERENCES

- [1] N. Inagaki, in *Proc. Japn. Symp. Plasma Chem.*, vol. 1, p297-302, 1988.
- [2] H. Yasuda, *J. of Polym. Sci. Macromolec, Rev.* 16, p199-293, 1981.
- [3] G.M.W. Kroesen, Plasma deposition: Investigations on a new approach, *Thesis*, Eindhoven University of Technology, 1988.
- [4] Y.L.M. Creyghton, *Internal report Eindhoven University of Technology, VDF-NT/89-03*, feb. 1989.
- [5] B. Dischler, R.E.Sah, P. Koidl, W. Fluhr, and A. Wokaun, Infrared and RAMAN analysis of hydrogenated amorphous carbon films prepared by RF plasma deposition from C_6H_6 or C_6D_6 vapor, in *Proc. 7th Int. Symp. Plasma Chemistry*, ed. by C.J. Timmermans, Eindhoven 1985, p45.